Coastal Engineering 65 (2012) 56–63

Contents lists available at SciVerse ScienceDirect

Coastal Engineering

journal homepage: www.elsevier.com/locate/coastaleng

On the parameterization of the free-stream non-linear wave orbital motion in nearshore morphodynamic models

B.G. Ruessink [a,*], G. Ramaekers [b], L.C. van Rijn [a,c]

[a] Institute for Marine and Atmospheric Research, Department of Physical Geography, Faculty of Geosciences, Utrecht University, P.O. Box 80.115, 3508 TC Utrecht, Netherlands
[b] Rijkswaterstaat Waterdienst, P.O. Box 17, 8200 AA Lelystad, Netherlands
[c] Deltares, P.O. Box 177, 2600 MH Delft, Netherlands

ARTICLE INFO

Article history:
Received 11 October 2011
Received in revised form 6 March 2012
Accepted 7 March 2012
Available online 4 April 2012

Keywords:
Velocity skewness
Velocity asymmetry
Wave-driven sand transport
Wave non-linearity

ABSTRACT

Nearshore morphodynamic models are computationally demanding, especially when the time scale of interest is weeks or longer. Hence, they often rely on a simple parameterization or non-linear wave theory to estimate the skewed-asymmetric shape of the near-bed, free-stream wave orbital motion, relevant to the prediction of onshore sand transport during mild wave conditions. Recently, Abreu et al. (2010) presented a simple analytical expression for this shape. Here, we present parameterizations to estimate the non-linearity parameter r and phase ϕ in this expression, such that the non-linear orbital motion can be estimated efficiently from values of the significant wave height H_s, wave period T, and water depth h, standard output of nearshore morphodynamic models. The parameterizations are based on a data set of 30.000+ field observations of the orbital skewness S_u and asymmetry A_u, collected under non-breaking and breaking wave conditions. Consistent with earlier observations, we find that the Ursell number, which includes H_s, T and h, describes the variability in S_u and A_u well and we use it to link H_s, T and h to r and ϕ. The comparison of our findings to another large field data set suggests that wave non-linearity depends weakly on wave directional spread and that our parameterizations may underestimate S_u for narrow-banded swell and (unidirectional) laboratory conditions. Furthermore, the use of the parameterizations is not advised on bed slopes steeper than in our data set (i.e., >1:30).

1. Introduction

As waves propagate from deep water onto beaches, their surface form and orbital water motion become increasingly non-linear because of the amplification of the higher harmonics. Initially, the waveform becomes asymmetric about the horizontal axis, with shorter, higher crests and longer, shallower troughs. This type of asymmetry is known as skewness and, for the orbital motion u in the direction of wave advance, is often quantified with the skewness parameter R_u (e.g., Ribberink and Al-Salem, 1994),

$$R_u = \frac{u_{\max}}{u_{\max} - u_{\min}}. \quad (1)$$

Because the maximum positive ('onshore') u, $u_{\max}$, exceeds the maximum negative ('offshore') u, $u_{\min}$, R_u exceeds 0.5. R_u is generally largest in the shoaling zone, and decreases as waves propagate further onshore and break. In the surf zone, the asymmetry about the horizontal axis changes into asymmetry about the vertical axis as the waves increasingly pitch forward, with a steep front face and a gentle rear face. This type of non-linearity, referred to as asymmetry, is related to the skewness of the derivative of u, the acceleration a (Elgar et al., 1997). Analogous to Eq. (1), velocity asymmetry can be described with the skewness parameter R_a (Watanabe and Sato, 2004),

$$R_a = \frac{a_{\max}}{a_{\max} - a_{\min}}. \quad (2)$$

Orbital motion with asymmetry only has $R_a > 0.5$ and $R_u = 0.5$. Velocity asymmetry can also be expressed as (Suntoyo et al., 2008)

$$\alpha = 2T_c/T, \quad (3)$$

where T_c is the duration between the negative-to-positive zero-crossing and $u_{\max}$, and T is the wave period. When R_a exceeds 0.5, α is less than 0.5. Under natural conditions, R_u typically varies between 0.5 and 0.7, and α between 0.2 and 0.5 (Elfrink et al., 2006).

Both velocity skewness and asymmetry generally result in onshore sand transport (e.g., O'Donoghue and Wright, 2004; Ribberink and Al-Salem, 1994; Ruessink et al., 2011; Van der A et al., 2010). This wave-induced transport results in onshore sandbar migration (e.g., Hoefel and Elgar, 2003; Hsu and Hanes, 2004; Ruessink et al., 2007) and contributes to beach accretion during mild wave conditions. An accurate description of the cross-shore evolution of the near-bed orbital motion is thus of crucial importance to nearshore waves–currents–bathymetric evolution (morphodynamic) models. Highly advanced deterministic wave models, such as those based on

* Corresponding author. Tel.: +31 302532780; fax: +31 302531145.
E-mail address: b.g.ruessink@uu.nl (B.G. Ruessink).

0378-3839/$ – see front matter © 2012 Elsevier B.V. All rights reserved.
doi:10.1016/j.coastaleng.2012.03.006

the Boussinesq or the Reynolds-Averaged Navier–Stokes equations, can nowadays provide this accurate description (e.g., Kennedy et al., 2000; Torres-Freyermuth et al., 2010); however, they are still too computationally demanding to be used in a morphodynamic setting, especially when the time scale of interest is days, weeks, or even longer. Furthermore, it is not a priori obvious that morphodynamic models including an advanced wave model result in more accurate predictions of beach evolution than models with a less advanced wave model because of the more pronounced accumulation of errors over time (Pape et al., 2010). Many operational morphodynamic models rely on simple parameterizations of the shape of the near-bed orbital motion. Initial parameterizations (e.g., Roelvink and Stive, 1989; Stive, 1986) considered velocity skewness only, but more recent parameterizations (e.g., Drake and Calantoni, 2001; Elfrink et al., 2006) consider velocity asymmetry as well, see Malarkey (2008) and Abreu et al. (2010) for reviews. Many of these parameterizations consider a limited number of higher harmonics or construct an orbital shape by patching together formulations for subsets of the waveform (e.g., from the zero up-crossing to u_{max}, etc.), which results in unrealistic acceleration time series. To overcome these shortcomings, Abreu et al. (2010) introduced a simple analytical expression for the free-stream near-bed horizontal orbital motion,

$$u(t) = U_w f \frac{sin(\omega t) + \frac{r sin\phi}{1+\sqrt{1-r^2}}}{1 - r\,cos(\omega t + \phi)}. \quad (4)$$

Here, t is time, $U_w = (u_{max} - u_{min})/2$ is the velocity amplitude, $\omega = 2\pi/T$, ϕ is a phase, r is a non-linearity measure and $f = \sqrt{1-r^2}$ is a dimensionless factor that ensures the amplitude of u to equal U_w. Eq. (4) is equivalent to $U_w \sum_{k=0}^{\infty} \frac{1}{n^k} sin[(k+1)\omega t + k\phi]$ with $r = 2n/(1+n^2)$. For $r = 0$, Eq. (4) describes sinusoidal flow. For $0 < r < 1$, it results in velocity-asymmetric flow for $\phi = 0$, velocity-skewed flow for $\phi = -\pi/2$, and mixed asymmetric-skewed flow for $-\pi/2 < \phi < 0$. Abreu et al. (2010) also outlined an approach how an (R,α) combination can be converted into an (r,ϕ) pair to estimate the near-bed orbital motion from Eq. (4). With this approach they found good agreement between synthetically generated and measured waves, with R and α determined from each individual measured wave. Motivated by this good agreement, Abreu et al. (2010) suggested that Eq. (4) can be included in nearshore bathymetric evolution models by using existing parameterizations for R_u and α (e.g., Dibajnia et al., 2001; Elfrink et al., 2006; Tajima and Madsen, 2002) to estimate r and ϕ and, hence, $u(t)$. Recently, Ruessink et al. (2009) and Ruessink et al. (2011) applied Eq. (4) to study the effect of wave non-linearity on sand transport.

The $u(t)$ form produced by Eq. (4) is monochromatic and it is not a priori clear whether its non-linearity is representative of a series of random, natural waves. To go from the time scale of a single wave to that of a series of waves, Elfrink et al. (2006) derived synthetic wave trains from statistical wave parameters such as the root-mean-square wave height and the duration of positive orbital motion, with the non-linearity of each individual wave determined from its height and period, the water depth, and the local bed slope. However, the time-averaged non-dimensional third-order moment of the synthetic wave trains compared poorly to field measurements. Thus, even though individual waves may be described rather accurately, error accumulation makes the use of a series of individual waves to estimate time-averaged measures of wave non-linearity questionable.

The aim of the present paper is to propose a new methodology to compute the non-linearity parameter r and phase ϕ in Eq. (4) from a representative wave height H, wave period T and water depth h such that the monochromatic $u(t)$ (i.e., Eq. (4)) has the velocity skewness and asymmetry representative of a series of random, natural waves. Our approach (Section **2**) is as follows. Firstly, we process a data set of ~34.000 time series of natural near-bed orbital motion into the third-order moments skewness S_u and asymmetry A_u (equations are given below). We prefer these two measures of wave-nonlinearity over R_u and α, as these latter two parameters are applicable to individual waves only. Secondly, we combine S_u and A_u into a measure of the total non-linearity B and a phase ψ. Thirdly, we follow Doering and Bowen (1995) and parameterize B and ψ in terms of the local Ursell number Ur, which is a function of H, T and h. Finally, we transform (B,ψ) into (r,ϕ). When applied in a morphodynamic model, our methodology thus combines a given H, T, and h into Ur, which in turn is used to estimate B and ψ, and finally, r and ϕ. Applications of our approach in the morphodynamic model of Van Rijn, (2007a,b) are also presented (Section **3**). Discussion and conclusions can be found in Sections **4** and **5**, respectively. We stress that our approach is not meant to replace the aforementioned advanced wave models; instead, it serves as a short-cut in practical engineering modeling where the use of these advanced models is not straightforward.

2. Parameterization

The data used here were collected during a series of subtidal and intertidal field campaigns at the barred beaches of Egmond aan Zee, Texel and Terschelling (all in The Netherlands) and of Truc Vert (France). The Dutch experiments comprise the Terschelling Nourtec campaigns executed between 1993 and 1995 (De Kruif and Rijks, 1998; Ruessink et al., 1998; Van Enckevort and Reincke, 1996), the Egmond Kust2000 and Coast3D campaigns in 1998 (Kroon and de Boer, 2001; Ruessink et al., 2001), the Egmond intertidal campaign in 2005 (Price and Ruessink, 2008), and the Texel Slufter intertidal campaign in 2009 (De Vries, 2010). The French experiment was conducted in spring 2008 at the Aquitanian Truc Vert beach (Ruessink, 2010). During all Dutch deployments, instantaneous (2 or 4 Hz) near-bed velocity and pressure recordings were made with a bidirectional electromagnetic flow (EMF) meter at a nominal height (depending on the experiment) between 0.1 and 0.5 m above the bed, and a pressure transducer (PT) between 0 and 2.2 m above the bed. During the French experiment, 10 Hz near-bed velocity and pressure was recorded with an acoustic Doppler velocimeter (ADV) with an internal PT between 0.1 and 1.3 m above the bed as bed level changed with time. Most measurements were carried out in burst mode, providing 2048 or 2400 s of data per hour. The ADV data comprised records of 24 min and 40 s each half hour. The data from the Egmond and Texel intertidal campaigns were recorded continuously, and processed in records of 15 min to ensure stationarity with respect to the changing tidal water level. All data blocks in which the PT, EMF, or ADV were temporarily dry were removed from the data, implying that our analysis below does not contain any data from the swash zone. The number of instrumented positions during each deployment ranged from 1 to 9. In total, 33.962 data records were available for further processing. The local bed slope at each measurement location was generally less than about 1:30.

All records of cross-shore and alongshore orbital velocity in the sea-swell frequency $f = 0.05 - 1$ Hz range were combined into time series of total sea-swell orbital velocity in the direction of wave advance, $u_w(t)$, using eigenfunction analysis. From each $u_w(t)$, the skewness S_u was computed as

$$S_u = \frac{\overline{u_w^3(t)}}{\sigma_{u_w}^3}, \quad (5)$$

where the overbar represents a time average and σ_{u_w} is the standard deviation of $u_w(t)$. The wave asymmetry A_u was also computed with Eq. (5), replacing $u_w(t)$ by its Hilbert transform (Elgar, 1987). With this definition, waves that pitch forward have negative A_u. Time series of the PTs were processed into water depth h, spectral significant sea-swell (frequency range 0.05 to 0.33 Hz) wave height H_s and period $T = m_{-1}/m_0$, where m_n is the spectral moment of order n. Subsequently, the Ursell number Ur was calculated as (Doering and Bowen, 1995),

$$Ur = \frac{3}{4}\frac{a_w k}{(kh)^3}, \quad (6)$$

with $a_w = 0.5H_s$ and k is the local wave number computed with linear wave theory using T. In our data, H_s ranged between 0.05 and 3.99 m,

T between 3.1 and 13.9 s, h between 0.25 and 11.2 m, and Ur between 0.004 and 24.8. If we take $H_s/h = 0.33$ as the outer edge of the surf zone (Ruessink et al., 1998), 31.4% of the data were collected under breaking wave conditions. 4.7% of the data had $H_s/h > 0.6$.

Fig. 1 shows S_u and A_u as a function of Ur. For $Ur < 0.04$, both S_u and A_u scatter around 0, indicating that the orbital motion is essentially sinusoidal. For $Ur > 0.04$, S_u initially increases to a maximum value of (on average) 0.63 at $Ur \approx 1-1.5$, then reduces to ≈ 0.2 for $Ur \approx 10$. For $Ur = [0.04-0.3]$, only S_u is non-zero, indicating a preponderance of large wave crests. For larger Ur, A_u steadily increases to ≈ -0.85 for $Ur \approx 10$, representing the change to pitched-forward waves. Although there is considerable scatter, there are no apparent groups of observations that are clearly at odds with other observations, neither for S_u nor for A_u. This implies that the variability in S_u and A_u is dependent primarily on the local h, H and T, and not on beach slope, as the Ursell number does not contain beach slope information. This is consistent with the findings of Kuriyama et al. (1990), Doering and Bowen (1995) and Elfrink et al. (2006) for the range of bed slopes considered here. The observed scatter may, in part, be due to variability in wind speed and direction (Feddersen and Veron, 2005) and in wave-directional spread (e.g., Janssen, 2006), see also Section **4** below.

The class-mean values of S_u and A_u were combined into a measure of the total (non-dimensional) non-linearity B,

$$B = \sqrt{{S_u}^2 + {A_u}^2} \tag{7}$$

and phase ψ,

$$\psi = tan^{-1}(A_u/S_u), \tag{8}$$

implying that $S_u = B cos\psi$ and $A_u = B sin\psi$. The dependence of B on Ur (Fig. 2a) suggests a fit in the form of a Boltzmann sigmoid,

$$B = p_1 + \frac{p_2 - p_1}{1 + exp\frac{p_3 - logUr}{p_4}}, \tag{9}$$

where p_1 and p_2 are the magnitude of B for $Ur \to 0$ and $Ur \to \infty$, respectively, p_3 is related to the deflection point, and p_4 is a measure of the slope. Using $p_1 = 0$ and a non-linear least-squares fitting procedure, we find $p_2 = 0.857 \pm 0.016$, $p_3 = -0.471 \pm 0.025$ and $p_4 = 0.297 \pm 0.021$, where the range represented by the $\pm$ values is the 95% confidence interval. For ψ we fit a *tanh*-function (Fig. 2b),

$$\psi = -90^\circ + 90^\circ tanh(p_5/Ur^{p_6}), \tag{10}$$

and find best-fit values $p_5 = 0.815 \pm 0.055$ and $p_6 = 0.672 \pm 0.073$.

Now that we have obtained empirical functions to relate Ur to B and ψ, the next step is to compute r and ϕ from B and ψ. B and r are related as (Malarkey and Davies, submitted for publication)

$$B = 3b/\sqrt{2(1-b^2)}, \tag{11}$$

with $b = r/\left(1 + \sqrt{1-r^2}\right)$. The phase ψ is related to ϕ as

$$\phi = -tan^{-1}(A_u/S_u) - \pi/2 = -\psi - \pi/2. \tag{12}$$

We summarize our approach with an example. The Battjes and Janssen (1978) wave transformation model was run with an offshore root-mean-square wave height of 1.5 m, a period of 8 s, shore-normal incidence, and a tidal water level of 0 m over the Egmond profile shown in Fig. 3i. At each grid point, the root-mean-square wave height H_{rms} (Fig. 3a), period T, and water depth h are known, which are combined into Ur (Fig. 3b) using Eq. (6) with $a_w = 0.5\sqrt{2}H_{rms}$. The non-linearity parameters B and ψ can subsequently be estimated with Eqs. (9) and (10), respectively (Fig. 3c and d),which, in turn, are converted to r and ϕ using Eqs. (11) and (12), see Fig. 3e and f. At each grid point, U_w can be estimated with linear wave theory (Fig. 3g), $U_w = \pi H_{rms}/Tsinh(kh)$. Finally, the estimates of r, ϕ and U_w are input into Eq. (4) to yield a monochromatic $u(t)$ at each grid point (Fig. 3h). These series can be used as input into an appropriate sand transport equation.

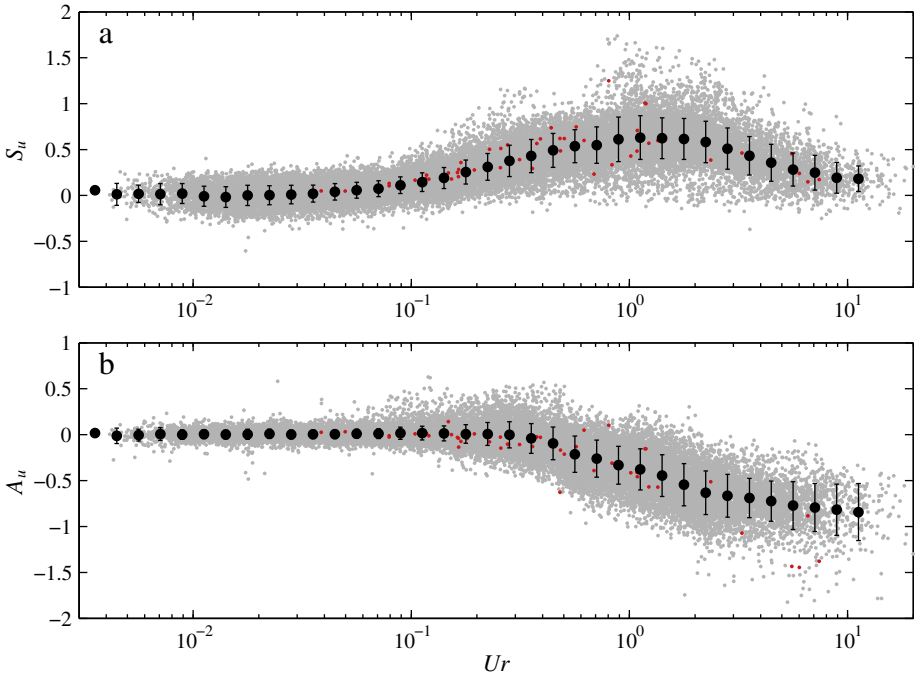

Fig. 1. (a) Near-bed velocity skewness S_u and (b) asymmetry A_u as a function of the Ursell number Ur. The gray dots are the 33.962 individual estimates, the filled circles are class-mean values based on binning the individual estimates according to $log(Ur) \pm 0.05$. The vertical lines represent $\pm$ one standard deviation in each bin. The 48 red dots are the data of Doering and Bowen (1995).

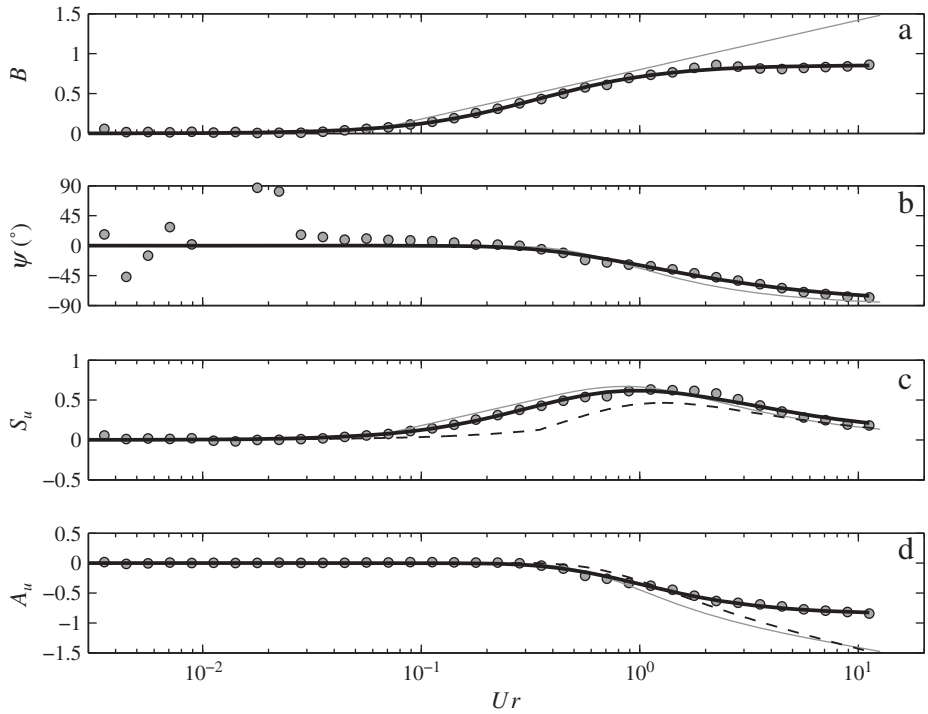

Fig. 2. Class-mean values (dots) and best-fit lines of the non-linearity parameter B, (b) phase ψ, (c) velocity skewness S_u, and (d) velocity asymmetry A_u as a function of the Ursell number Ur. The black lines in (a)–(d) are the best-fit lines. The gray lines in all panels are fits proposed by Doering and Bowen (1995): (a) $B = 0.8 + 0.62log(Ur)$, (b) $\psi = -90° + 90°tanh(0.73/Ur)$, (c) $S_u = Bcos(\psi\pi/180)$ and (d) $A_u = Bsin(\psi\pi/180)$. The dashed line in (c) is the S_u parameterization proposed by Kuriyama (2009). The dashed line in (d) is the A_u dependence on Ur we deduced from Kuriyama (2009)'s S_u parameterization.

3. Application

The proposed parameterization was embedded in the cross-shore morphological CROSMOR model (Van Rijn, 2007a,b). It can be chosen as an alternative to the Isobe and Horikawa (1982) method, which combines fifth-order Stokes with third-order cnoidal wave theory and can yield skewed and asymmetric orbital wave motion. The Isobe and Horikawa (1982) method was recently described extensively in Abreu et al. (2010), and is therefore not reiterated here. In the CROSMOR model, the effect of the skewness and asymmetry of the near-bed orbital motion is implemented in the bedload equation. The original version of this equation dates back to Van Rijn (1984, 2007a) modified it to include asymmetry effects on sand transport by incorporating the approach of Nielsen (2006).

The aim of this section is to illustrate the effect of the new parameterization on nearshore morphological change, compared to the previous Isobe and Horikawa (1982) approach. To this end, the CROSMOR model was run with both approaches for 5 days with the initial profile shown in Fig. 4c, a time-invariant offshore root-mean-square wave height of 1 m and peak period of 10 s, and semi-diurnal (tidal) water level variations with a range of 1.1 m. The initial profile is based on a profile measured during the Duck94 experiment at Duck, N.C. (e.g., Gallagher et al., 1998; Hoefel and Elgar, 2003), the field experiment that sparked much of the recent interest in the effect of velocity asymmetry on sand transport. The median grain size was set to 350 μm. Fig. 4a illustrates the peak onshore and offshore near-bed orbital velocities – default CROSMOR output – estimated by both approaches for the initial profile. As can be seen, differences in the peak onshore velocity are minimal. Across the sandbar, the peak offshore velocity estimated with the Isobe and Horikawa (1982) remains approximately constant, while that estimated with the new approach shows a more pronounced water depth dependence. This illustrates that the velocity skewness produced by the Isobe and Horikawa (1982) approach is considerably larger than that computed with the new methodology. The same difference can be seen near the shoreline; the peak onshore and offshore orbital velocity in the new approach are about equal, indicating a dominance of velocity asymmetry, while with the Isobe and Horikawa (1982) approach the velocity skewness is unrealistically pronounced. Apparently, the Isobe and Horikawa (1982) approach does not correctly reduce velocity skewness for high Ur.

Fig. 4b shows that both the bed load and suspended load are affected by the choice of velocity parameterization. For the bed load a difference was expected as the bed load is directly affected by the shape of the near-bed orbital motion. The suspended load is affected because the two parameterizations yield different orbital shapes, and hence bed shear stress and reference (near-bed boundary) concentrations to solve the advection–diffusion equation used to estimate the suspended load. For both approaches, the net (i.e., the sum of the bed load and suspended load) transport is onshore and peaks seaward of the bar crest, resulting in onshore bar migration and growth (Fig. 4c). As the cross-shore gradients in bed load are predicted to be more pronounced with the new parameterization, the bar height has grown more as well (Fig. 4c). The runs were repeated with a median grain size of 200 μm and the same wave and water level forcing. In this case, the seaward-directed suspended load was predicted to be slightly larger than the shoreward-directed bed load and the sandbar moved offshore. Again, after 5 days, the sandbar was more pronounced with the new velocity parameterization than with the Isobe and Horikawa (1982) approach (Fig. 4d), although the difference in bar height is less than in the 350 μm simulation. The model simulations presented here thus indicate that the primary effect of the new velocity parameterization is to induce larger gradients in cross-shore sand transport (compared to that predicted with Isobe and Horikawa (1982)), which, for the two cases examined here, results in more pronounced bar growth during both onshore and offshore bar migration.

4. Discussion

In this section we compare our findings to the existing S_u and A_u parameterizations proposed by Doering and Bowen (1995) and

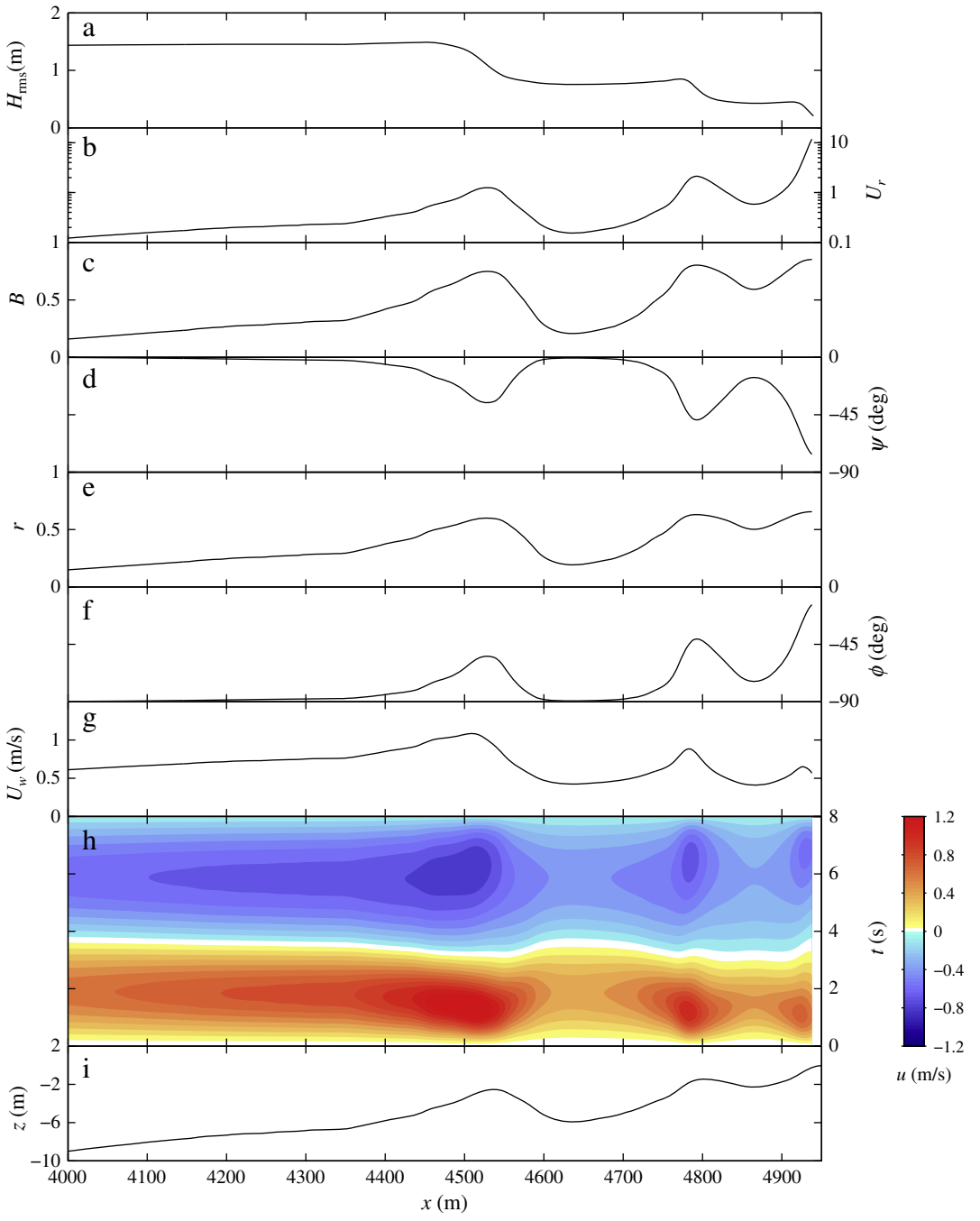

Fig. 3. (a) Root-mean-square wave height H_{rms}, (b) Ursell number Ur, (c) non-linearity parameter B, (d) phase ψ, (e) non-linearity parameter r, (f) phase ϕ, (g) velocity amplitude U_w, (h) horizontal orbital motion $u(t)$ and (i) bed elevation z versus cross-shore distance x. $z=0$ corresponds to mean sea level. The wave model was initialized at $x=0$ in about 16-m water depth.

Kuriyama (2009) and to the Ur dependence of S_u and A_u in the Duck94 data set.

Fig. 2 also contains the Doering and Bowen (1995) fits for B, ψ, S_u and A_u, based on their 48 data points shown in Fig. 1. These and our fits differ primarily for Ur in excess of ~3. In the Doering and Bowen (1995) fit, B increases linearly with $log(Ur)$, whereas in our fit B saturates at about 0.9. Also, the Doering and Bowen (1995) ψ is slightly closer to -90° for high Ur. Both differences have minimal effect on S_u (Fig. 2c), but cause A_u to increase faster with Ur for $Ur>3$ than in our data (Fig. 2d); however, it is obvious from Fig. 1 that the high-Ur behavior of the Doering and Bowen (1995) fits was based on four data points only, while our data comprised 2.218 observations with $Ur>3$. Their four points fall within the scatter of our data.

Kuriyama (2009) combined Doering and Bowen (1995)'s parameterization for S_u with his own S_u fit based on data collected at Hasaki, Japan (Kuriyama et al., 1990). We note that Kuriyama et al. (1990) and Kuriyama (2009) used the non-linearity parameter $\Pi=kH_s/(2\pi)coth^3(kh)$; in shallow water, Π is proportional to Ur, $Ur=3\pi\Pi/4$. On the whole, his S_u values fall below those of Doering and Bowen (1995)'s and our parameterization (Fig. 2c). Kuriyama et al. (1990) based his original fit on S_u values computed from u_w series including infragravity waves (i.e., including $f<0.05$ Hz), while we restricted ourselves to the sea-swell frequency range. When we compare his sea-swell S_u (Fig. 6 in Kuriyama et al., 1990) to our observations, we find that both data sets largely overlap, implying that the difference in Fig. 2c is due to a difference in the computational method (see also Appendix B in Kuriyama (1991)). Kuriyama (2009) did not propose

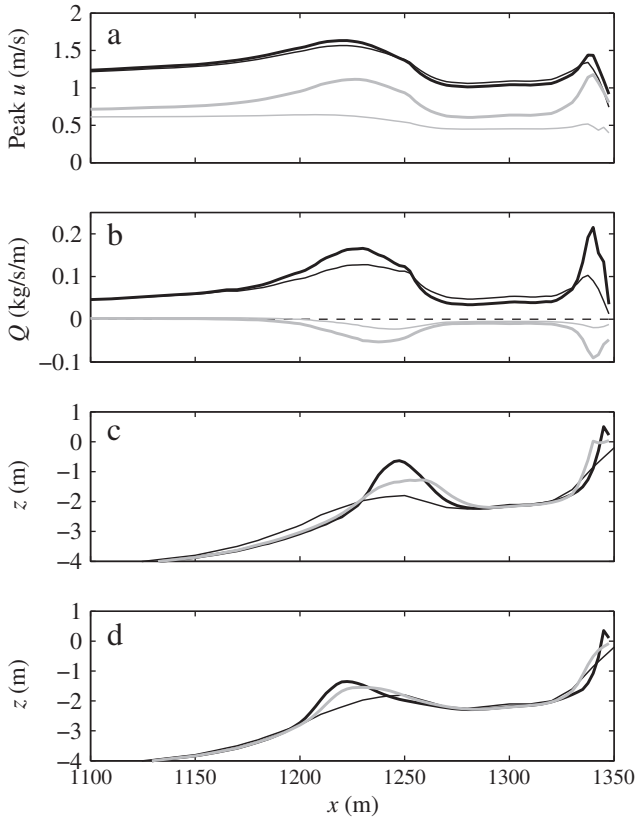

Fig. 4. (a) Peak onshore (black lines) and offshore (gray lines) orbital velocity predicted by the Isobe and Horikawa (1982) method (thin) and our approach (thick) and (b) bedload (black lines) and suspended load (gray lines) with the Isobe and Horikawa (1982) method (thin) and our approach (thick) versus cross-shore distance x at time = 0. In (b), the dashed line is zero transport. (c) and (d) show predicted morphological evolution after 5 days with the Isobe and Horikawa (1982) method (gray) and our approach (black) using a median grain size of 350 μm and 200 μm, respectively. In (c) and (d), the thin black line is the initial profile. $x = 0$ corresponds to the most seaward grid location in 10-m depth.

an A_u parameterization (instead, he focused on the acceleration skewness) but his S_u fit allows to construct the A_u curve shown in Fig. 2d. The Ur dependence of A_u is similar to that of Doering and Bowen (1995). Kuriyama et al. (1990) did not have any data for $Ur > 5$.

The Duck94 data used here was collected between August 10 and November 3, 1994 at Duck, N.C., using 13 co-located EMF (nominal height of 0.5 m above the bed) and PT sensor-combinations positioned in a cross-shore array from approximately 8-m depth to just seaward of the swash zone. All measurements were collected continuously with a sampling frequency of 2 Hz and were processed here in blocks of 1 h. In total, 17.134 data blocks were processed, with Ur in the 0.005–15 range, comparable to our data set. The S_u and A_u Duck94 values broadly show the same Ur-dependence as our values, compare Fig. 5 with Fig. 1; however, there are differences. While in our data only 1.1% of all values had $S_u > 1$, in the Duck94 data this was 8.7%. In more detail, the Duck94 S_u is, on average, larger than in our data set for $Ur > 0.6$ (Fig. 5a). A similar difference is not notable for A_u (Fig. 5b). Note that also the Duck94 A_u does not increase as profoundly with Ur for high Ur as suggested by Doering and Bowen (1995) and Kuriyama (2009). Although there is considerable scatter, Fig. 6 suggests that S_u is negatively related to the sea-swell directional spread s_θ, here estimated with a principal component analysis of the (u,v) matrix (s_θ corresponds to the square root of the relative contribution of the second eigenvector to the total variance). The larger S_u are limited to situations with $s_\theta < 15-20°$ in both data sets. Because the Duck94 data set contains considerably more data points with $s_\theta < 15°$ (30.8% at Duck versus 13.1% in our data for the Ur selection shown in Fig. 6), Su is, on average, higher in the Duck94 data set for the same Ur, causing the overall differences seen in Fig. 5a. The differences in s_θ characteristics may be due to the fact that our data were collected primarily in sea-dominated settings; the Duck94 data contains more narrow-banded swell conditions. If we extrapolate the dependence of S_u on s_θ to unidirectional ($s_\theta = 0$) laboratory conditions, we may expect that the fits proposed here will underestimate S_u in laboratory settings. Analogously, the dependence of S_u on s_θ implies that models that compare well to measures of wave non-linearity in the laboratory, may not necessarily perform well when applied to field situations. The weak dependence of wave non-linearity on the directional characteristics of the primary waves is qualitatively consistent with earlier laboratory observations (Elgar et al., 1993) and theoretical considerations (Janssen, 2006), and is likely due to the weakening of the energy transfer from the primary-wave frequencies to their higher harmonics with an increase in directional spread (Janssen, 2006, and references therein). Why here the directional spread affects skewness but not asymmetry, is not understood.

5. Conclusions

We have extended the work of Doering and Bowen (1995) and Kuriyama (2009) by developing a new methodology to compute a monochromatic time series of the free-stream, near-bed orbital velocity from a representative wave height, wave period and water depth such that it has the velocity skewness and asymmetry representative of a series of random, natural waves. Our methodology is based on the analysis of 30.000+ data blocks of 2–10 Hz near-bed orbital velocities collected in the field and links the wave height, period and water depth through the Ursell number to a measure of wave non-linearity and phase in the orbital-velocity expression of Abreu et al. (2010). We believe that our approach is particularly relevant for nearshore morphodynamic models that aim to predict nearshore evolution on time scales of weeks and longer, for which advanced deterministic

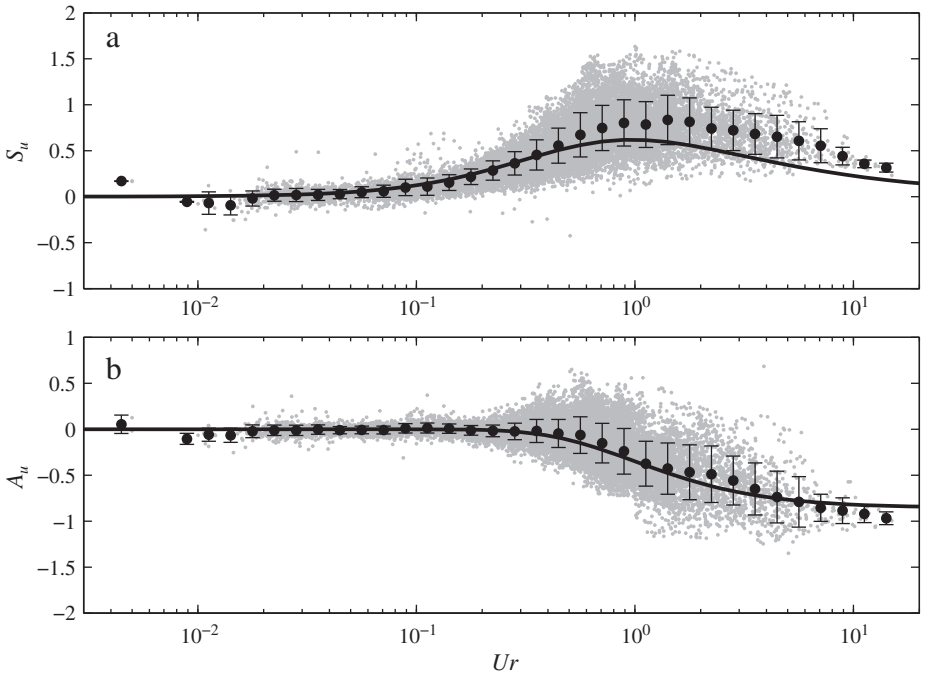

Fig. 5. (a) Near-bed velocity skewness S_u and (b) asymmetry A_u as a function of the Ursell number Ur for the Duck94 data. The gray dots are the 17.134 individual estimates, the filled circles are class-mean values based on binning the individual estimates according to $log(Ur) \pm 0.05$. The vertical lines represent $\pm$ one standard deviation in each bin. The thick black lines are the best-fit S_u and A_u, respectively, based on Eqs. (**9**) and (**10**).

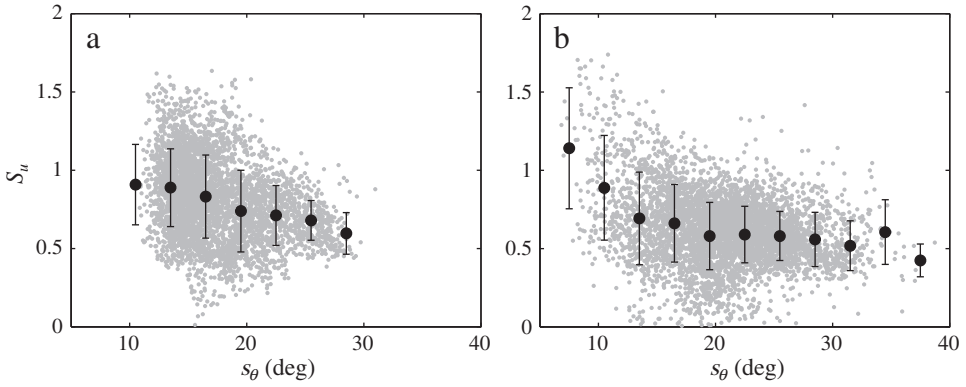

Fig. 6. Near-bed velocity skewness S_u in the $Ur = 0.75 - 2$ range versus sea-swell directional spread s_θ in (a) the Duck94 data and (b) the data used in Section 2. The gray dots are the individual estimates, 4.239 in (a) and 5.107 in (b). The filled circles are class-mean values based on binning the individual estimates according to $s_\theta \pm 4$. The vertical lines represent $\pm$ one standard deviation in each bin. The $Ur = 0.75 - 2$ range was chosen here because in this range S_u is approximately independent of Ur, see Figs. 1a and 5a.

wave models are too computationally demanding. In the operational Van Rijn (2007a,b)'s CROSMOR model, the new parameterization results in more pronounced bars during both onshore and offshore migration, compared to predictions using the Isobe and Horikawa (1982) methodology. The parameterizations of non-linearity and phase we propose here are based predominantly on directionally spread sea conditions, and may underestimate the skewness of orbital velocity in narrow-banded (in direction) swell and unidirectional laboratory waves. Furthermore, the use of the parameterizations is not advised on bed slopes steeper than in our data set (i.e., $> 1:30$).

Acknowledgments

We are greatly indebted to all students, staff members and technicians involved in the collection of the field observations. The Dutch observations were collected in the framework of a number of national and international projects, including KUST*2000, NOURTEC and Coast3D, funded by Rijkswaterstaat and the EU, respectively. The French observations were collected within the structure of the multi-institutional ECORS (SHOM-DGA) project. The field observations from Duck were collected by R.T. Guza and Steve Elgar with funding from the Office of Naval Research and the National Science Foundation. We thank Dr. J. Malarkey for providing insight into the analytical relation between B and r, Eq. (11). This paper is a contribution to the BarBec project (ANR N2010 JCJC 602 01), coordinated by Bruno Castelle at EPOC, University of Bordeaux I.

References

Abreu, T., Silva, P.A., Sancho, F., Temperville, A., 2010. Analytical approximate wave form for asymmetric waves. Coastal Engineering 57, 656–667.
Battjes, J.A., Janssen, J.P.F.M., 1978. Energy loss and set-up due to breaking of random waves. Proc. 16th Int. Conf. on Coastal Engineering. ASCE, New York, pp. 570–587.

De Kruif, A., Rijks, D., 1998. Morphological and hydrodynamical characteristics of an intertidal bar and trough system. Master's thesis, Department of Physical Geography, Faculty of Geosciences, Utrecht University.
De Vries, J.J., 2010. Infragravity wave behaviour in a secondary tidal inlet, the Slufter, the Netherlands. Master's thesis, Department of Physical Geography, Faculty of Geosciences, Utrecht University.
Dibajnia, M., Moriya, T., Watanabe, A., 2001. A representative wave model for estimation of nearshore local transport rate. Coastal Engineering Journal 43, 1–38.
Doering, J.C., Bowen, A.J., 1995. Parameterization of orbital velocity asymmetries of shoaling and breaking waves using bispectral analysis. Coastal Engineering 26, 15–33.
Drake, T.G., Calantoni, J., 2001. Discrete particle model for sheet flow sediment transport in the nearshore. Journal of Geophysical Research 106, 19859–19868.
Elfrink, B., Hanes, D.M., Ruessink, B.G., 2006. Parameterization and simulation of near bed orbital velocities under irregular waves in shallow water. Coastal Engineering 53, 915–927.
Elgar, S., 1987. Relationships involving third moments and bispectra of a harmonic process. IEEE Transactions on Acoustics, Speech, and Signal Processing ASSP-35, 1725–1726.
Elgar, S., Guza, R.T., Freilich, M.H., 1993. Observations of nonlinear interactions in directionally spread shoaling surface gravity waves. Journal of Geophysical Research 98, 20299–20305.
Elgar, S., Guza, R.T., Raubenheimer, B., Herbers, T.H.C., Gallagher, E., 1997. Spectral evolution of shoaling and breaking waves on a barred beach. Journal of Geophysical Research 102, 15797–15805.
Feddersen, F., Veron, F., 2005. Wind effects on shoaling wave shape. Journal of Physical Oceanography 35, 1223–1228.
Gallagher, E.L., Elgar, S., Guza, R.T., 1998. Observations of sand bar evolution on a natural beach. Journal of Geophysical Research 103, 3203–3215.
Hoefel, F., Elgar, S., 2003. Wave-induced sediment transport and sandbar migration. Science 299, 1885–1887.
Hsu, T.J., Hanes, D.M., 2004. Effects of wave shape on sheet flow sediment transport. Journal of Geophysical Research 109. doi:10.1029/2003JC002075.
Isobe, M., Horikawa, K., 1982. Study on water particle velocities of shoaling and breaking waves. Coastal Engineering in Japan 25, 109–123.
Janssen, T.T., 2006. Nonlinear surface waves over topography. Ph.D. thesis, Technical University of Delft, The Netherlands.
Kennedy, A.B., Dalrymple, R.A., Kirby, J.T., Chen, Q., 2000. Determination of inverse depths using direct Boussinesq modeling. Journal of Waterway, Port, Coastal, and Ocean Engineering 126, 206–214.
Kroon, A., de Boer, A., 2001. Horizontal flow circulation on a mixed energy beach. Proc. Coastal Dynamics'01. ASCE, New York, pp. 548–557.
Kuriyama, Y., 1991. Investigation on cross-shore sediment transport rates and flow parameters in the surf zone using field data. : Tech. Rep., 31(2). Port and Harbour Research Institute, pp. 3–58.
Kuriyama, Y., 2009. Numerical model for bar migration at Hasaki, Japan. In: Mizuguchi, M., Sato, S. (Eds.), Proc. Coastal Dynamics 2009. : No. Paper 50. World Scientific. published on CD-ROM.
Kuriyama, Y., Katoh, K., Isogami, T., 1990. Wave nonlinearity and cross-shore sediment rate in the vicinity of breaker zone. Proceedings of Coastal Engineering. JSCE, pp. 284–288 (in Japanese).
Malarkey, J., 2008. A review of freestream descriptions and velocity and acceleration skewness. Tech. Rep. SANTOSS UWV Internal Report Number 2, Bangor University.
Malarkey, J., Davies, A.G., submitted for publication. Free-stream velocity descriptions under waves with skewness and asymmetry. Coastal Engineering.
Nielsen, P., 2006. Sheet flow sediment transport under waves with acceleration skewness and boundary layer streaming. Coastal Engineering 53, 749–758.
O'Donoghue, T., Wright, S., 2004. Flow tunnel measurements of velocities and sand flux in oscillatory sheet flow for well-sorted and graded sands. Coastal Engineering 51, 1163–1184.
Pape, L., Kuriyama, Y., Ruessink, B.G., 2010. Models and scales for nearshore sandbar behavior. Journal of Geophysical Research 115, F03043. doi:10.1029/2009JF001644.
Price, T.D., Ruessink, B.G., 2008. Morphodynamic zone variability on a microtidal barred beach. Marine Geology 251, 98–109.
Ribberink, J.S., Al-Salem, A.A., 1994. Sediment transport in oscillatory boundary layers in cases of rippled beds and sheet flow. Journal of Geophysical Research 99, 12707–12727.
Roelvink, J.A., Stive, M.J.F., 1989. Bar-generating cross-shore flow mechanisms on a beach. Journal of Geophysical Research 94, 4785–4800.
Ruessink, B.G., 2010. Observations of turbulence within a natural surf zone. Journal of Physical Oceanography 40, 2696–2712.
Ruessink, B.G., Houwman, K.T., Hoekstra, P., 1998. The systematic contribution of transporting mechanisms to the cross-shore sediment transport in water depths of 3 to 9 m. Marine Geology 152, 295–324.
Ruessink, B.G., Miles, J.R., Feddersen, F., Guza, R.T., Elgar, S., 2001. Modeling the alongshore current on barred beaches. Journal of Geophysical Research 106, 22451–22463.
Ruessink, B.G., Kuriyama, Y., Reniers, A.J.H.M., Roelvink, J.A., Walstra, D.J.R., 2007. Modeling cross-shore sandbar behavior on the timescale of weeks. Journal of Geophysical Research 112, F03010. doi:10.1029/2006JF000730.
Ruessink, B.G., van den Berg, T.J.J., van Rijn, L.C., 2009. Modeling sediment transport beneath skewed asymmetric waves above a plane bed. Journal of Geophysical Research 114, C11021. doi:10.1029/2009JC005416.
Ruessink, B.G., Michallet, H., Abreu, T., Sancho, F., van der A, D.A., van der Werf, J.J., Silva, P.A., 2011. Observations of velocities, sand concentrations, and fluxes under velocity-asymmetric oscillatory flows. Journal of Geophysical Research 116, C03004. doi:10.1029/2010JC006443.
Stive, M.J.F., 1986. A model for cross-shore sediment transport. Proc. 20th Int. Conf. on Coastal Engineering. ASCE, New York, pp. 1550–1564.
Suntoyo, Tanaka, A., Sana, H., 2008. Characteristics of turbulent boundary layers over a rough bed under saw-tooth waves and its application to sediment transport. Coastal Engineering 55, 1102–1112.
Tajima, Y., Madsen, O.S., 2002. Shoaling, breaking and broken wave characteristics. Proc. 28th Int. Conf. on Coastal Engineering. World Scientific, Singapore, pp. 222–234.
Torres-Freyermuth, A., Lara, J.L., Losada, I.J., 2010. Numerical modelling of short- and long-wave transformation on a barred beach. Coastal Engineering 57, 317–330.
Van der A, D.A., O'Donoghue, T., Ribberink, J.S., 2010. Measurements of sheet flow transport in acceleration-skewed oscillatory flow and comparison with practical formulations. Coastal Engineering 57, 331–342.
Van Enckevort, I.M.J., Reincke, E., 1996. Longshore currents in the intertidal zone of Terschelling. IMAU Report V96.09. Utrecht University.
Van Rijn, L.C., 1984. Sediment transport. Part I: bed load transport. Journal of Hydraulic Engineering 110, 1431–1456.
Van Rijn, L.C., 2007a. Unified view of sediment transport by currents and waves, I: initiation of motion, bed roughness and bed-load transport. Journal of Hydraulic Engineering 133, 649–667.
Van Rijn, L.C., 2007b. Unified view of sediment transport by currents and waves, II: suspended transport. Journal of Hydraulic Engineering 133, 668–689.
Watanabe, A., Sato, S., 2004. A sheet-flow transport rate formulations for asymmetric, forward-leaning waves and currents. Proc. 29th Int. Conf. on Coastal Eng. ASCE, New York, pp. 1703–1714.